

## Some advantages of shear interferometry for gas-dynamic investigations

Sergey I. Inshakov<sup>1\*</sup>, Sergey I. Klimentyev<sup>2</sup>, Andrey Yu. Rodionov<sup>2</sup>, Valentin N. Shekhtman<sup>2</sup>

<sup>1</sup> State Research Center "The Central Aerohydrodynamic Institute" (TsAGI),  
140181, Zhukovsky, Moscow region, Russia

<sup>2</sup> Engineering & Physics Laboratory (EFL Ltd.),  
box 26, 196608, Pushkin 8, Saint-Petersburg, Russia

\*corresponding author: sergin55@mail.ru, 140181, Zhukovsky, Moscow region, Zhukovsky str. 1

---

**Abstract** Shear interferometric and shadow methods can be applied for the small-scale gas flows structure study, including turbulence characteristics. Shear interference and shadow patterns are often used to visualize the gas flow at small shear values and with maximum possible fringe width. Nevertheless mentioned patterns intensity spatial modulation contains various information especially about the flow statistical characteristics. This paper analyzed differences between the information contained in shear interferograms and shadow patterns. Mentioned difference is illustrated by modeling experimental data

**Keywords:** Shear interferometry, Toepler shadow method, gas-dynamic, turbulence, turbulence spectrum, interference pattern processing, spatial spectrum, wave front, Fourier spectra, vibration resistance.

---

### Introduction

Shear interferometric and shadow methods (Toepler method) represent a gas flow structure visualization and thermodynamic parameters distribution investigation instrument. Shear interferogram and shadow pattern look often determined by gas-dynamic medium integral density distribution along the testing beam as a reference light beam interferometric system. At the same time in several cases reference light beam interferometric systems has informational advantage over shear interferometry and shadow methods in terms of the equal sensitivity to gas-dynamic medium different inhomogeneity scales. However reference light beam interferometric system tested implementation is an extremely complicated technical problem due to their high vibration sensitivity especially in cases of large scale stands. Moreover high-speed gas flow inhomogeneity and test object dimensions often lead to multiple breaks and contrast loss of interference fringes. In this case, mentioned interference pattern disadvantages practically can not be removed or compensated due to unregulated reference light beam interferometric systems sensitivity. Shadow methods are widely used to transparent inhomogeneity study including gas-dynamic medium due to mentioned reference light beam interference systems disadvantages.

This paper submits comparative shadow method and shear interferometry capabilities demonstration in gasdynamic studies. These capabilities are illustrated not so much shadow and interferometry methods well-known mathematical description analysis as the calculation models and experimental data demonstration. This approach seems more rewarding during the preliminary experiment planning, for example in turbulent gas flows study.

Shadow systems most prevalent on the gas dynamic study stands because of vibration resistance and density distribution picture visual perception accessibility, especially the flow around models. Obtained with shadow patterns gas-dynamic medium density distribution reconstruction yield shear interferometry on results accuracy and density inhomogeneity spatial resolution as shown below despite researchers great attention of shadow patterns quantitative interpretation [1, 2]. In addition, shear interferometric method has the distinct advantage allowing to change interferometric system sensitivity and thus get available for quantitative processing interference pattern type with large density gradients. This fact greatly expands measurements dynamic range from slightly density inhomogeneous gas-dynamic medium to shock of the flows. However, informational limitations should take into account using shear interferometry systems. They determine embodiment and measurement methods specifics to fill the missing information including gas-dynamic medium thermodynamic parameters.

At least three uncertainties («information loss types») should be taken into account in the shear interferogram wave-front shape reconstruction results, [3, 4, 5].

**Direction dependent sensitivity**

First information loss type related to the fact that it's impossible to predict wave front function behavior in the orthogonal shear vector direction by shear interferogram form. For example, cylindrical and parabolic wave fronts are impossible to distinguish on the lateral shear interferogram. Indeed, for these distortion types wavefront functions correspond:

$$\varphi_p(x, y) = A \cdot (x^2 + y^2) / (2 \cdot R); \quad \varphi_z(x, y) = A \cdot x^2 / (2 \cdot R),$$

and corresponding to the shear interferograms difference functions will have the same form:

$$\psi_x(x, y) = \varphi(x, y) - \varphi(x + s, y) = A \frac{x \cdot s}{R},$$

here  $A$  – normalizing factor,  $s$  - shear value.

Instrument sensitivity anisotropy to the knife direction appears less in the shadow method. Shear and shadow method phase distortions registration systems numerical modeling done to illustrate this feature. Harmonic phase grating distortion model type was used as the phase distortion:

$$\varphi(x, y) = \sin \left[ 2\pi \left( \frac{x}{T_x} + \frac{y}{T_y} \right) \right] \tag{1}$$

where  $T_x, T_y$  – harmonic modulation period along the transverse coordinates.

Shadow instrument optical scheme is shown in Fig.1, and shear interferometer - in Fig.2.

Wave takes place at the entrance of both measurement systems represented in the calculation of the complex amplitude  $A(x, y) = A_o \exp(ik\varphi(x, y))$ . Telescopic system with magnification equal to one accepted for systems Fig.1 and Fig.2 giving entrance pupil of diameter  $D$  image in the detection plane. In this intensity and phase uniform light wave  $\varphi(x, y)$  expected in the entrance pupil plane spaced a distance of  $4 \cdot f$  from the image plane.

Measuring systems radiation propagation calculation made by solving the parabolic wave equation in paraxial approximation. Thus the light field complex amplitude distribution  $A_1(x, y)$  determined on the shadow instrument and shearing interferometer exit pupil simulating a real shadow or shear pattern.

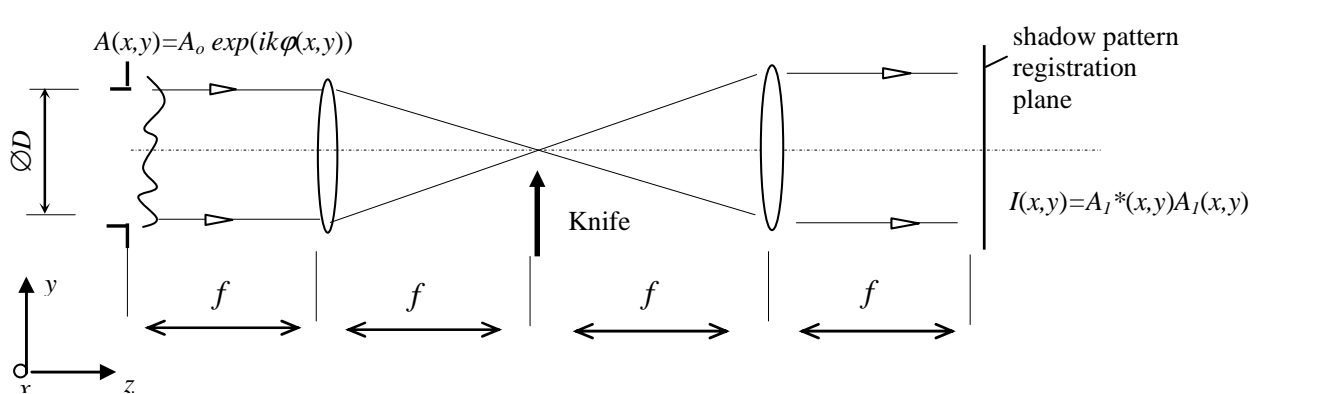


Fig.1 Shadow instrument scheme

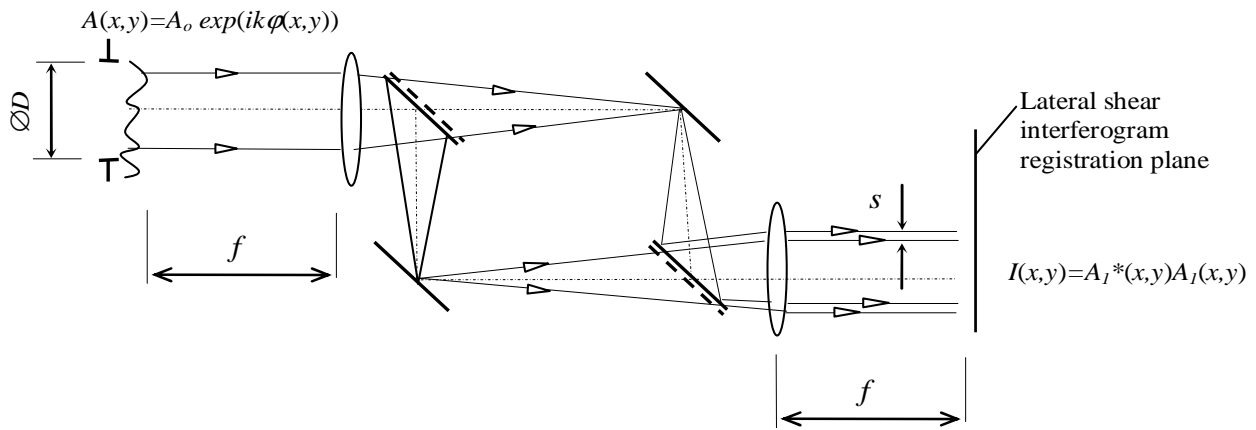


Fig.2 Lateral shear interferometer scheme

Fig.3 shows the shear interferograms and shadow patterns for the two harmonic distortion orientations. Distortions entered in the calculation program description and other information about the model experiment are given below the figure. Informativity both shear interferometric and shadow systems depends strongly on the relative orientation of the probing the medium wave phase modulation gradient vector and shear direction or shadow instrument knife edge illustrated modulated wavefront intensity distribution shown on Fig.3. Sensitivity anisotropy may result to complete signal loss, for example, with mutually perpendicular phase modulation gradient direction or mutually parallel image shear and knife edge. Recording with two noncollinear shear vectors and knife directions has to carry out to this information loss problem. For example, two mutually orthogonal shear vectors  $s_x$  and  $s_y$  interferogram commonly used in the case of lateral shear interferometer.

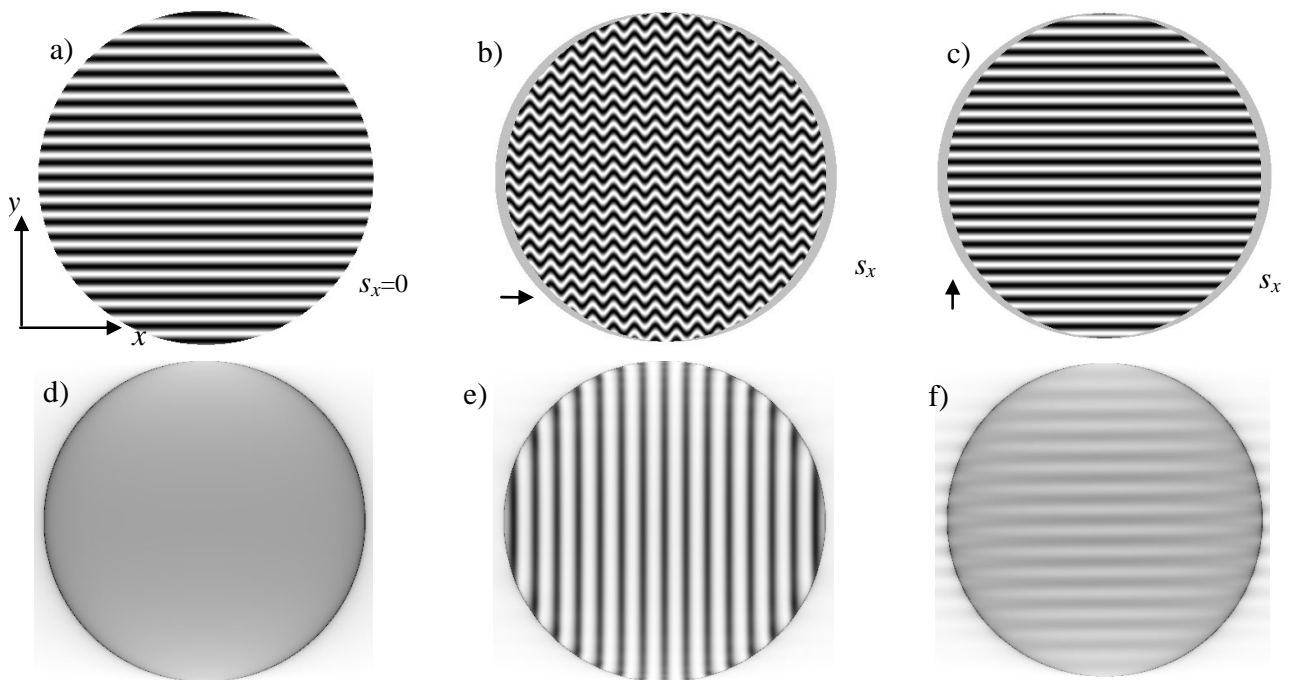


Fig.3 Lateral shear interferograms (a, b, c) and shadow patterns (d, e, f) with different orientation harmonic inhomogeneities (arrow on b and c):

b) and e):  $\varphi(x, y) = \sin\left[2\pi\left(\frac{x}{T_o}\right)\right]$ ;    c) and f):  $\varphi(x, y) = \sin\left[2\pi\left(\frac{x}{100 \cdot T_o} + \frac{y}{T_o}\right)\right]$ ;

spatial period –  $T_o=D/20$ ; interferogram image shear b) and c) –  $s_x = D/40$ ;

a) – lateral shear interferometer configuration image;

b) – shear interferogram maximum signal in case of  $s_x = 0,5 \cdot T_o$ ;

c) – signal absence for orthogonal directions of phase modulation gradient and shear;

d) – exit pupil plane radiation intensity distribution in the absence of knife;

e) – knife edge is perpendicular to phase modulation gradient (parallel to shadow pattern intensity modulation stripes);

f) – knife edge is parallel to phase modulation gradient, additional harmonic entered to indicate parallel to intensity stripes knife edge position.

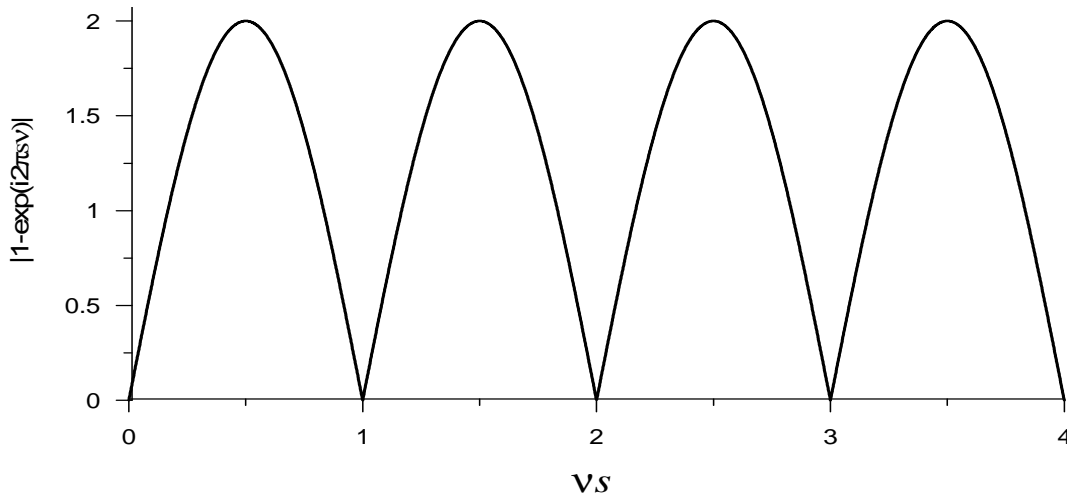


Fig.4 Lateral shear interferometer transfer function modulus graph.

### Spatial frequencies selective sensitivity

Second data loss type associated with shear interferometers selective sensitivity to a wavefront deformation spatial frequencies, including complete sensitivity loss at certain frequencies [5, 6]. So in the case of lateral shear difference function Fourier spectra  $\psi(x) = \varphi(x) - \varphi(x-s)$  and wavefront function  $\varphi(x)$  (one dimension case is sufficient) are related to each other:

$$H(\nu) = \Phi(\nu) \cdot [1 - \exp(-i2\pi\nu s)] \quad (2)$$

$$H(\nu) = F[\psi(x)], \quad \Phi(\nu) = F[\varphi(x)]$$

where F – Fourier transform operator.

Function  $\Omega(\nu) = [1 - \exp(-i2\pi\nu s)]$  represents the lateral shear interferogram transfer function.

Function modulus graph  $\Omega(\nu)$  presented in Fig.4.

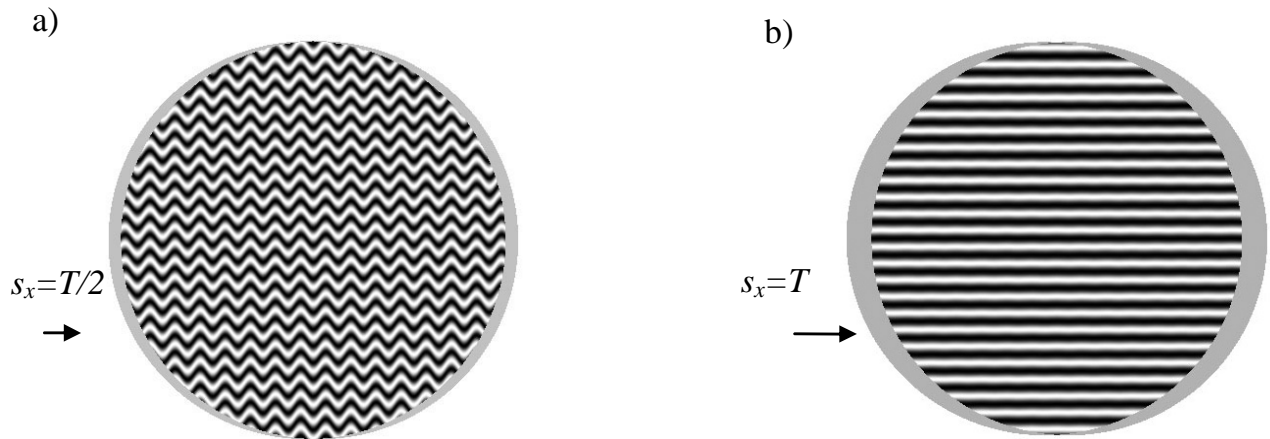
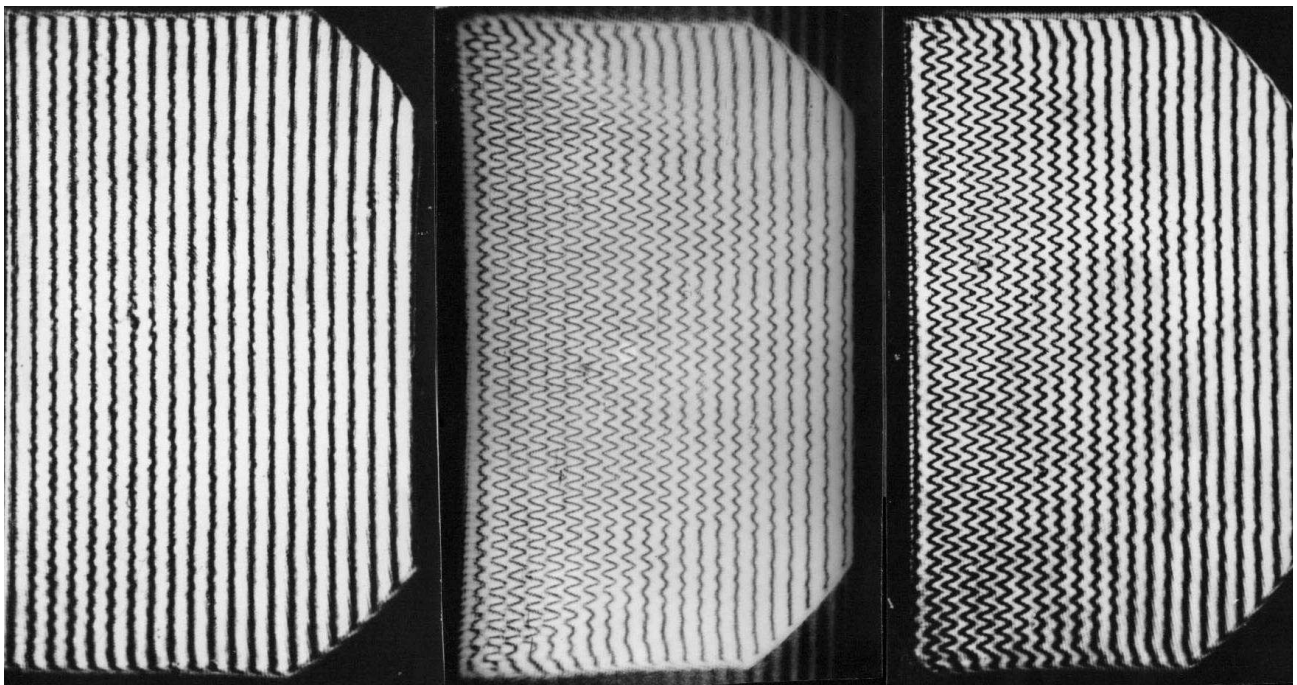


Fig.5 Lateral shear interferograms of test object  $\varphi(x, y) = \sin \left[ 2\pi \left( \frac{x}{D/20} \right) \right]$ , for two shear values of  
 a)  $s = (D/40)$ ; b)  $s = (D/20)$



a) b) c)

Fig.6 Nozzle array shear interferograms

Fig.6 shows two-dimensional flow interferograms after a "flat" constant step nozzle grid. Lateral shear interferometer sensitivity is a function with a period of  $1/s$  as shows expressions (2) and Fig.4. Wave function distortion amplitude information on the shear interferogram is completely absent at frequencies  $\nu = n/s$ ,  $n = 0, 1, \dots$  however double sensitivity compared to the same object reference wavefront interferogram takes place on frequencies  $\nu = (n + 0,5)/s$ ,  $n = 0, 1, \dots$ . For example, Fig.5 shows calculated shear interferogram models: in Fig.5a shear is half of the harmonic distortion period, in Fig.5b shear is equal to the harmonic distortion period. On the interferogram a) shear is equal to nozzle array step; b) – shear is half of the harmonic nozzle array step, i.e. condition  $\nu \cdot s = 0,5$  is satisfied; c) – shear value is intermediate  $0 < \nu \cdot s < 0,5$ . Testing object joint two interferogram processing with a nonmultiple collinear lateral shear values allows avoiding information loss at a shear multiple spatial frequencies [5, 6]. Another second type information loss

compensation option is possible for specific gas-dynamic medium like the study of isotropic turbulence spectrum gas-dynamic medium, for example, using radial and reverse shear interferometers. Wavefront spectrum can be represented as a spectra linear combination obtained by two shear interferogram processing in case of nonmultiple shear value two interferogram registration. Thus joint spatial spectral informativity of the two interferograms  $H_1(v)$  и  $H_2(v)$  can be expressed as:

$$\Phi(v) = \frac{H_1(v) \cdot |1 - \exp(-i2\pi s_1 v)| + H_2(v) \cdot |1 - \exp(-i2\pi s_2 v)|}{|1 - \exp(-i2\pi s_1 v)| + |1 - \exp(-i2\pi s_2 v)|} \quad (3)$$

Second type information loss could be almost completely eliminated with proper, shear  $s_1$  и  $s_2$  selection. As an example, Fig.7 shows spectral "sensitivity" interference system graph (proportional to the weight function), obtained with two shear values  $s$  and  $1.093s$ .

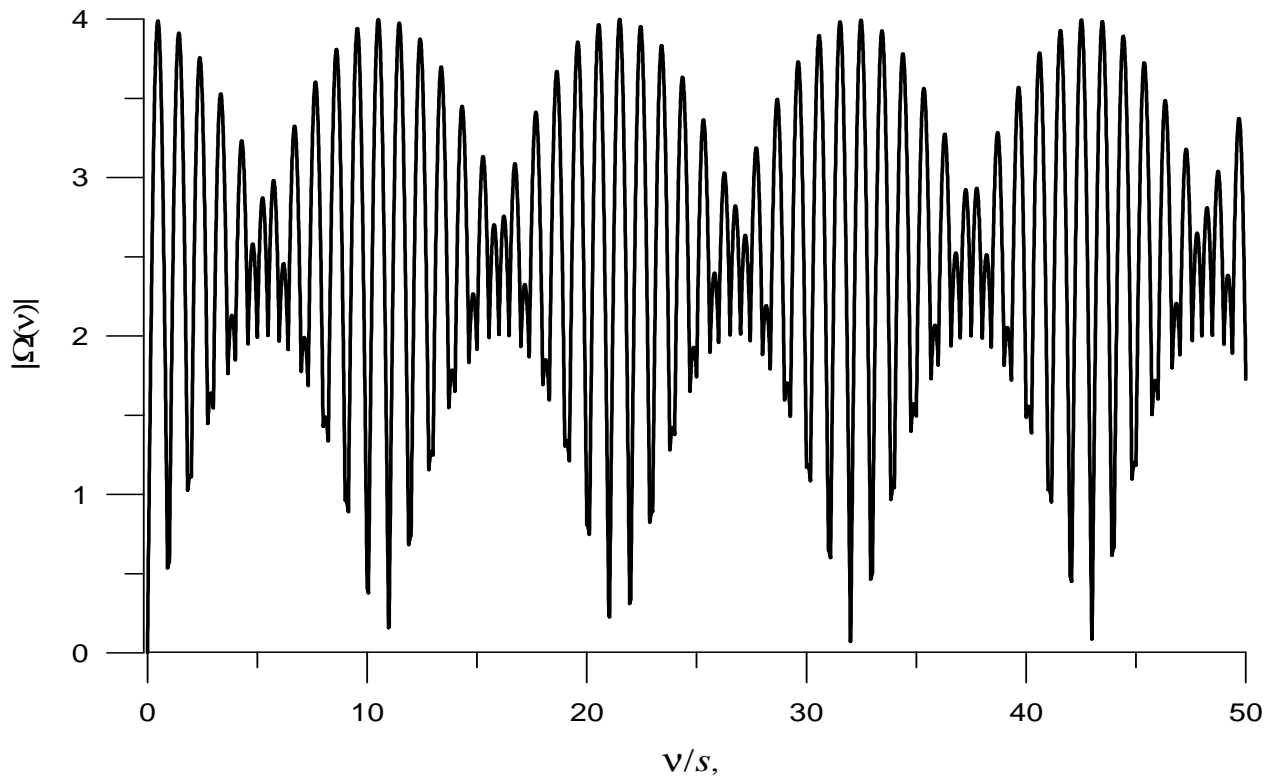


Fig.7 Lateral shear interferometer spectral spatial "sensitivity" graph for joint interferogram processing with the shear value of  $s$  and  $1.093s$ .

Spatial frequencies bandwidth may have a complex shape for shadow instruments as well as shear interferometers. signal frequency spectrum is explicitly regulated by the knife-edge position for considering scheme variant, Fig.1. Any knife-edge displacement causes corresponding harmonics complete loss due to knife-edge screening or the phase contrast loss due to positive and negative signal frequencies passing. Shadow patterns corresponding to the knife displacement in the Fourier plane shown in Fig.8. Shadow pattern contrast becomes nearly zero at the knife offset value more than instrument Fourier plane

$$\delta = \frac{\lambda f}{(D/20)} \text{ linear harmonic coordinates as shown on Fig.8.}$$

Such a dependence on the knife-edge setting accuracy may adversely affect the measurements quality since the optical wedge appearance in the flow (that is common) causes test beam translational amplitude distribution displacement in the Fourier plane and, consequently, information loss about the number of flow

phase distortion frequency components.

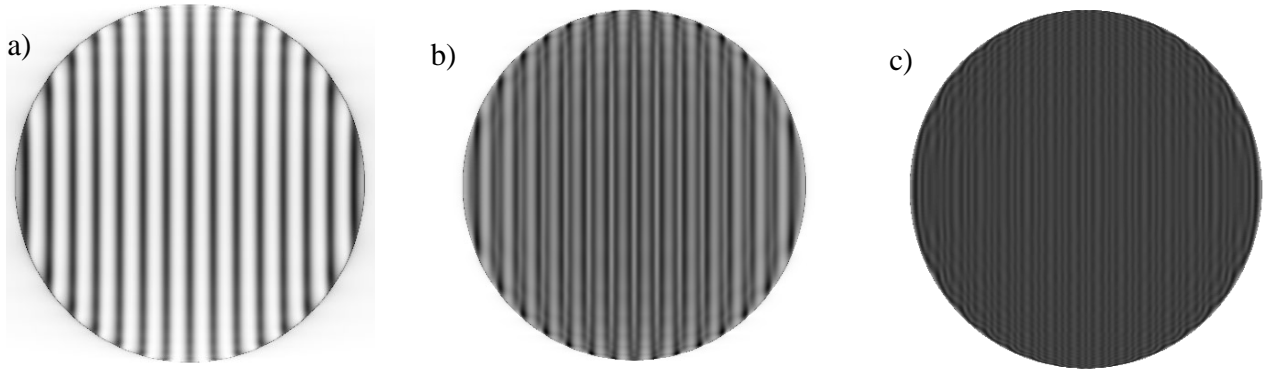


Fig.8 Shadow patterns, obtained with harmonic wavefront distortion  $\varphi(x, y) = \sin\left[2\pi\left(\frac{x}{D/20}\right)\right]$  for knife edge

offset equal to a)  $\Delta=0$ ;    b)  $\Delta = 0.6 \frac{\lambda f}{(D/20)}$  ;    c)  $\Delta = 1.2 \frac{\lambda f}{(D/20)}$ .

### Incomplete object image filling

The third information loss type caused by incomplete filling investigated object image by interference pattern characteristic only for the shear interferometers. For the spatially restricted beams expression (1) takes the form:

$$\Psi'(v) = \Phi'(v) \cdot [1 - \exp(-i2\pi s v)] + L(v), \quad (4)$$

where:

$$\Psi'(v) = \cdot F[\psi'(x)]; \quad \Phi'(v) = F[\varphi'(x)];$$

$$\psi'(x) = \begin{cases} \psi(x) & x \in [s, D] \\ 0 & \text{all other cases} \end{cases}$$

$$\varphi'(x) = \begin{cases} \varphi(x) & x \in [0, D] \\ 0 & \text{all other cases} \end{cases}$$

$$L(v) = -\int_0^s \varphi(x) \cdot \exp[-i2\pi vx] dx + \exp[-i2\pi vs] \int_{D-s}^D \varphi(x) \cdot \exp[-i2\pi vx] dx$$

where D – beam aperture.

Unlike the "infinite" aperture case function  $\varphi'(x)$  has nonzero values only in the beam aperture area [0, D], and function  $\psi'(x)$  - in the interference field of sheared relative to each other beams, i.e. recorded investigated object image [0, s] part does not contain the interference pattern.

Expression (4) can be used to reconstruct the lateral shear interferograms wave front, if function L(v) is known. As shown in [4] this function can be determined if there is a priori wave front behavior information on any beam aperture interval length equal to the shear vector value s. The absence of this information leads to the wavefront information distortions discrecity with a step equal to the shear value, i.e. unambiguous wavefront restoration is possible in a discrete points set with a spatial step equal to the shear s.

In contrast to the optical shop testing tasks mentioned part of the object in the segment [0, s] usually contains an interference pattern in the flow study. Gas-dynamic medium under study density distribution can be reconstructed on the interferogram without the third information loss type disadvantages if this image element is undisturbed flow part.

### Systems comparison

Important measuring system characteristics are the precision and measurement dynamic range besides instrument sensitivity anisotropy and transfer function. According to these parameters interferometric systems have a significant advantage over the shadow instruments.

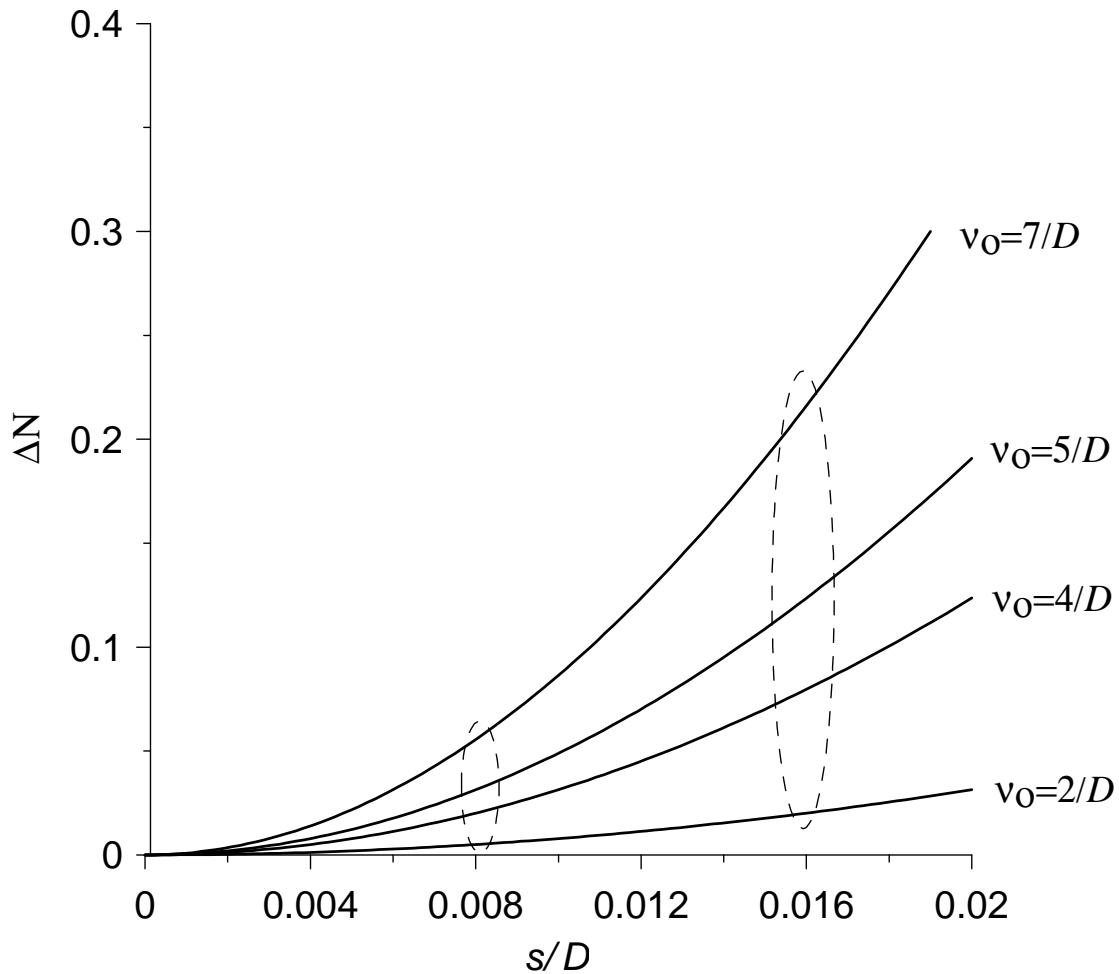


Fig.9 Interference fringe displacement dependency for different spatial frequencies  $v_0$  harmonic phase distortion from relative shear value.

Fig.9 presents interference bands displacement dependence (expressed as a bandwidth fraction) of the shear value for different harmonic frequency phase perturbations. As you can see, the transition from the shear  $s/D = 1.6\%$  to  $s/D = 0.8\%$  average interferometer sensitivity falls almost four times.

This feature allows adjusting the shear interferometers for the a priori known gas flow characteristics. In principle, this allows (which appears in the interference fringes gap particularly in reference wavefront interferometers) to obtain quantitative information even with the supersonic flows shock without loss of information [7]. Can be see in Fig.10 flow regions, separated by such shock. However, the shear value selection has yielded quantitative areas density relation of shock-divided flow.

By the shear variation can be adjusted the amount of displacement of the interference fringe corresponding to density gradient in the flow. On the interference pattern obtained by use the reference wave front on the shock wave is a gap interference fringe. In this case the ratio of the density on the shock wave can be approximately determined from the slope of the shock front. It is assumed that before the shock wave are known, at least two of the thermodynamic parameters of the medium. In the use of shearing interferometer reduction magnitude of the shear can be used to establish a correspondence fringes before and after the shock wave.

Figure 10 shows the interferogram shear flow of the active medium of  $\text{CO}_2$ -laser. The dimensions of the flow: along the optical axis of the probe light beam - 1850mm; in the vertical direction in the plane of the



drawing - 90mm.

The magnitude of the shear in the interference patterns 10a and 10c provides identification of fringes before and after the shock wave (for each interferogram shows an enlarged view of the selected rectangle area). Increased shearing interferogram 10b, resulting in a higher sensitivity of the measurement system, but it becomes problematic identification strips on both sides of the shock wave. Interferogram 10a was obtained from a ruby laser, and 10c of He-Ne laser. Almost the identical resolution of fringes on these interferograms illustrates vibrostability of interferometric system.

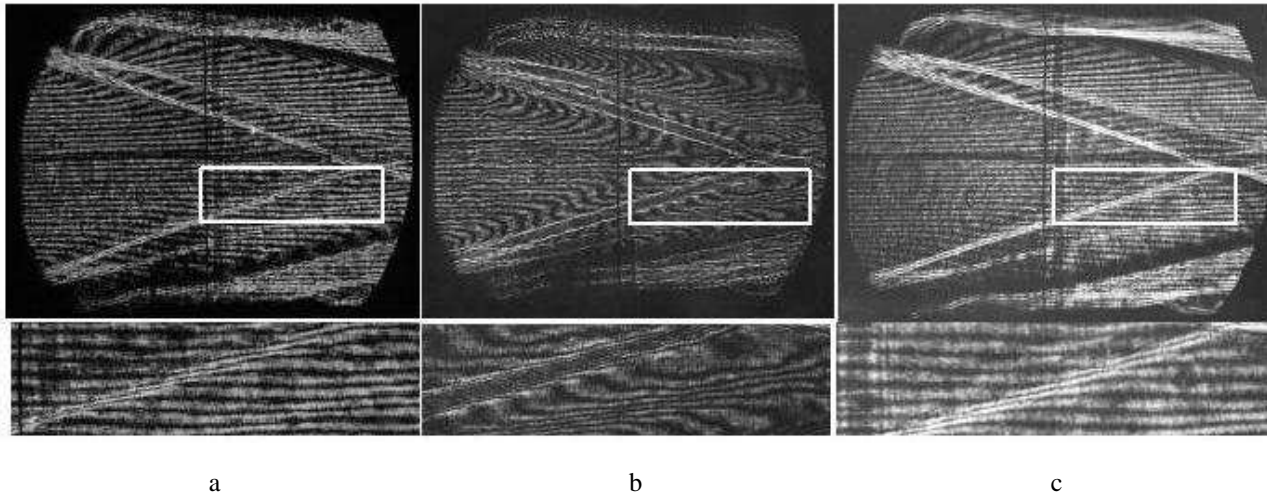


Fig.10

The shadow instruments quantitative measurements dynamic range is noticeably inferior to shear systems. Fig.11 shows comparison testing beam calculated image intensity distribution obtained for the two measuring systems by varying the phase harmonic distortion amplitude.

Shadow patterns quantitative processing error exceeds such of shear interferograms due to the detected signal parameters difference. In shadow pattern processing each detector pixel records the total intensity determined by adding the testing different aperture part light beams where gas dynamics medium is observed. In the shear pattern fringe displacement characterizes the phase difference between similar aperture sections. Moreover specified shear interferogram property reduces the demands to the detecting camera linearity and to the amplitude noise presence on the interference pattern.

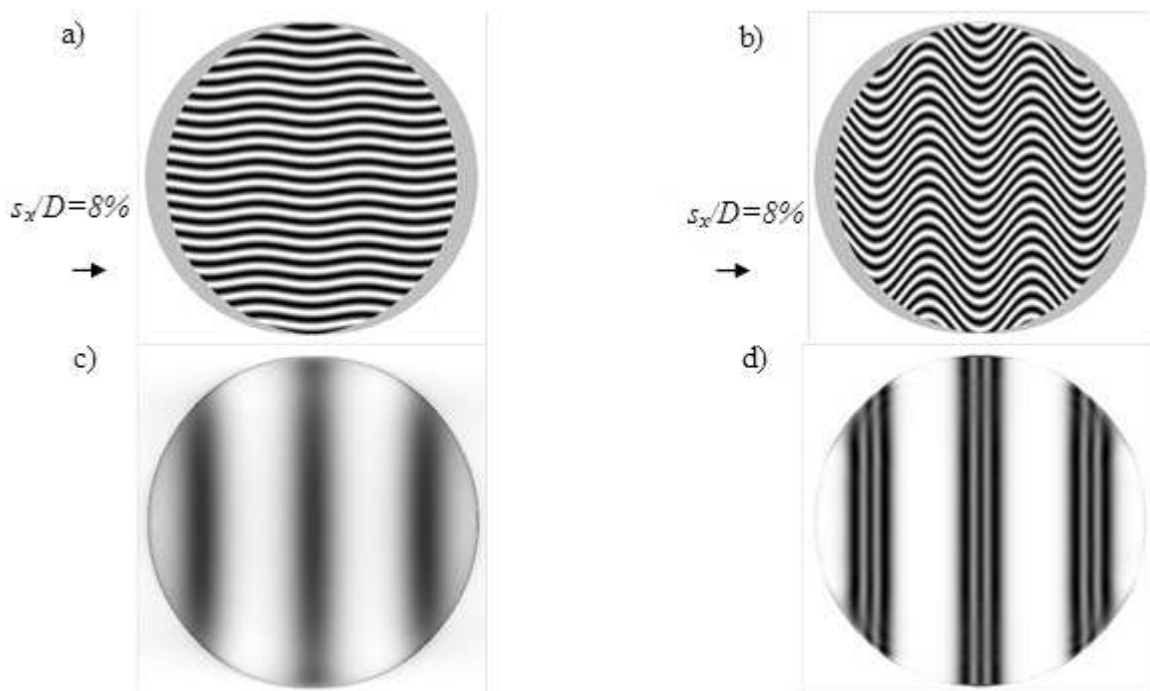


Fig.11 Shear (a,b) and shadow (c,d) calculated patterns obtained by testing the harmonic phase inhomogeneities

$$\varphi(x, y) = \phi \sin \left[ 2\pi \left( \frac{x}{D/4} \right) \right] \text{ where } \phi = 1 \text{ (a,c) and } \phi = 8 \text{ (b,d).}$$

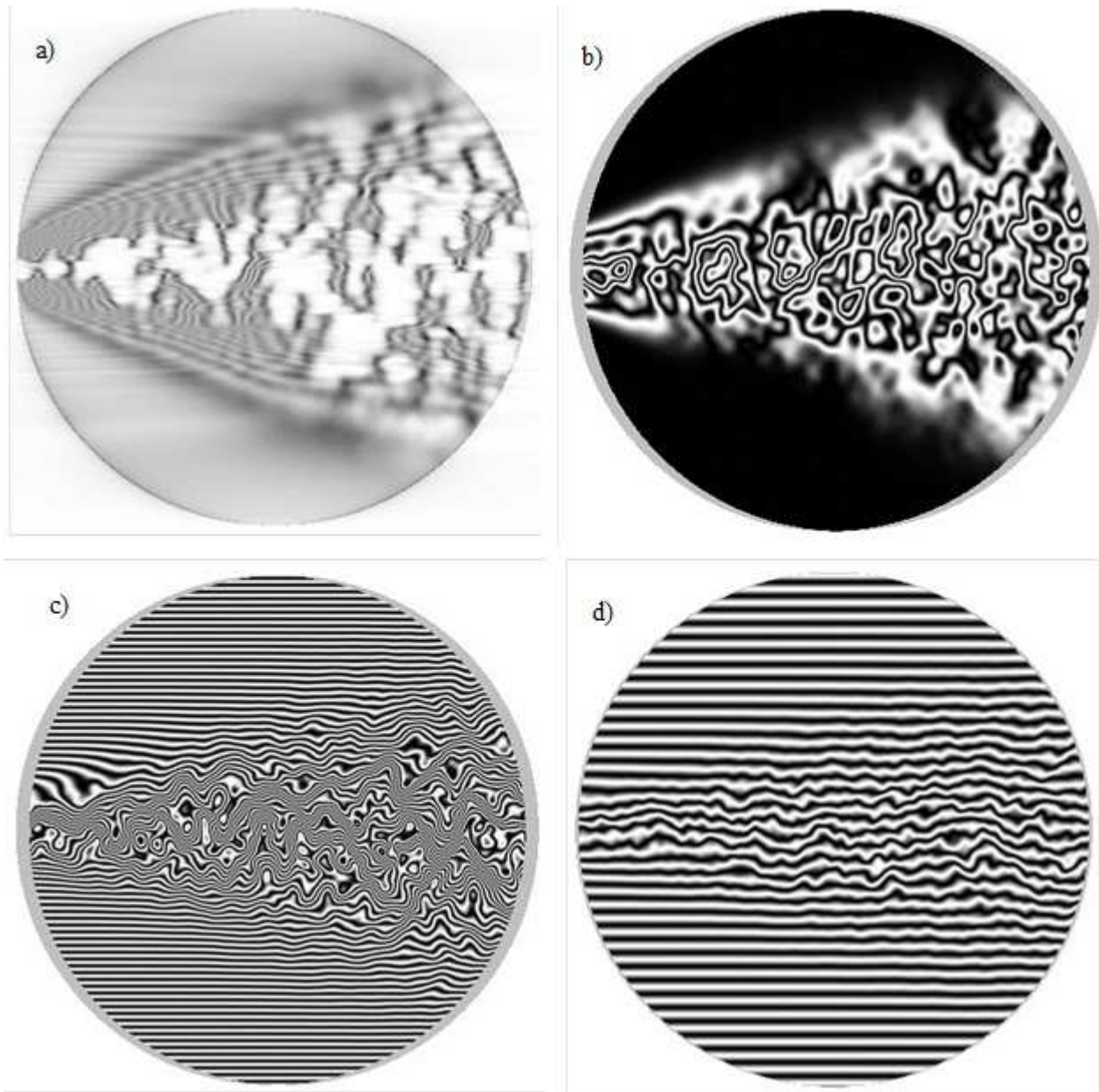


Fig.12 Shadow (a) and shear (b,c,d) calculated gas flow model patterns

Fig.12 illustrates differences between shadow and shear interference patterns in resolution of refractive index random distribution structure details in a gasdynamic medium.

Shear interference and shadow patterns are used mainly for gas flows visualization at low shear values and highest possible fringe width. Fig.12 shows the numerical simulation result of turbulent gas flow with shadow instrument (Fig.12a) and shear interferometer with "infinitely" wide interference fringe (Fig.12b). Finite fringe mode (Fig.12c) allows obtaining specific information about the density distribution in some flow sections.

Adjusting shearing interferometer dynamic range allows to fully getting a gas-dynamic medium density distribution quantitative results by setting testing object image shear (Fig.12d).

### Some realizations

This paper introduce modernization options of perhaps the best lateral shear interferometer schematic

solution IT-183 interferometer. Similar light-splitting unit configuration devices modification mainly consists in: compact and stable laser light sources; interferogram registration CCD cameras latest development; remote interference patterns and measurement process settings control electronic techniques. These tools usage in IT-183 interferometer design represents one of the shearing interferometer modernization examples including IT-144 и IT-228 as the IT-183 created in State Optical Institute and led by A.A. Zabelin performed by EFL Ltd. on assignment of TsAGI.

**Interferometric systems based on IT-183**

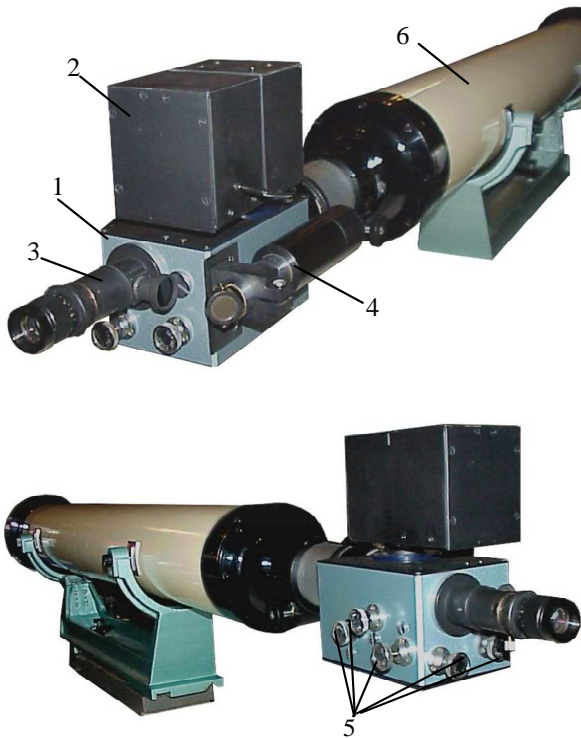


Fig.13 Pulsed source interferometric system.

- 1- IT-183 shearing interferometer;
- 2- light source unit; 3- viewing tube; 4- CCD matrix unit;
- 5- interferometer adjustment handles; 6- collimator

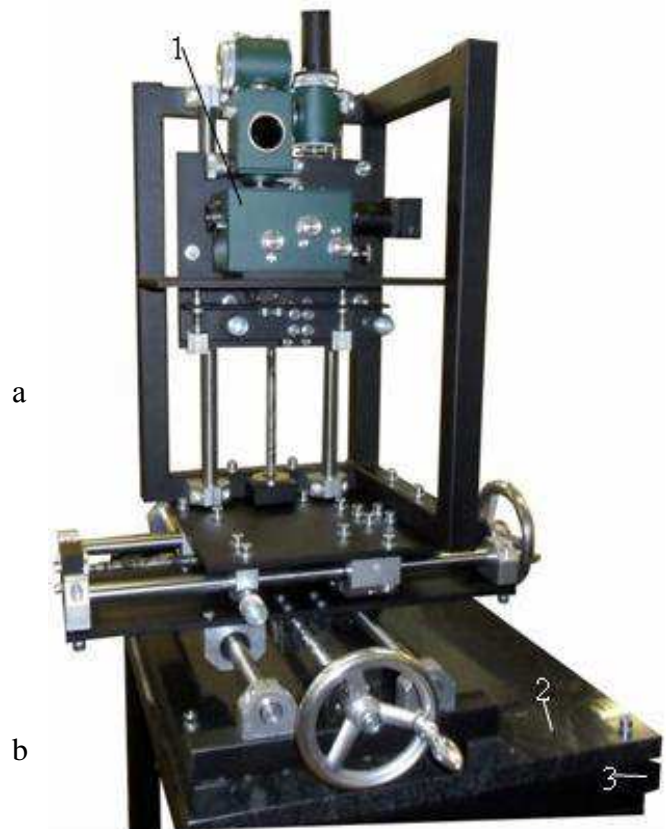


Fig.14 IT-183 on the amortized coordinate basis.

- 1- IT-183 shearing interferometer; 2 and 3- gabrodiabaz plates;

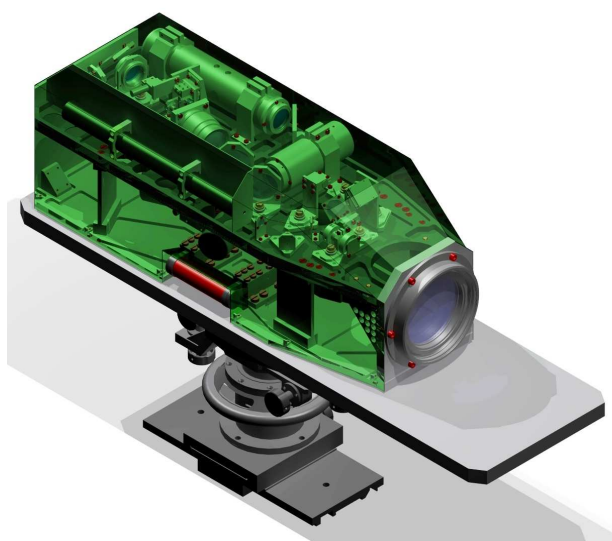
IT-183 interferometer based single unit interferometric system designed and made, Fig.13, for gasdynamic, chemical and electric-discharge lasers active media inhomogeneity measuring. Pulsed laser designed by EFL Ltd installed as a light source. Laser yttrium aluminum active element radiates at a 1.064 microns wavelength. 8 ns duration pulse is formed with a passive shutter. Case located light source power supply unit consists of capacitive accumulator and pump lamp closed discharge module. 635nm wavelength emitting semiconductor laser diode placed in the same casing. Object visual observation viewing tube saved in interferometric system shown in Fig.13. New CCD camera models permit to use computer screen image for small shear values measuring. That's why viewing tube presence and recording images on film become less relevant now. Beam splitter outputs viewing tube light beam and image rendered on the matrix with a pair of lenses.

Examined flow along and perpendicular moving interferometric system supporting structure produced for the interferometer IT-183 and a spherical autocollimation mirror interferometric system. Interferometer and mirror movement along the optical axis provided for system alignment. Fig.14 shows supporting structure

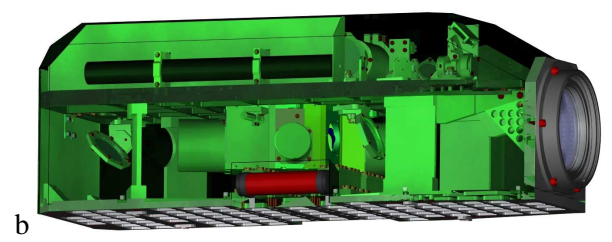
with the installed interferometer, pos.1. Gabrodiabaz plate, pos.2, based on similar plate, pos.3, via shock tool. Ballast load construction attached to plate pos.2. This construction do not contact plate pos.3, and it's center of gravity maximally close to the base plane. Along the axis movement amplitude of the aerodynamic channel – 600mm; in perpendicular vertical direction – 500mm and along the horizontal direction – 300m Interferometer base plate fixed using two-axis joint (Hooke joint) and fixed by a thrust screw. Upgraded IT-183 interferometer equipped with CCD camera optically conjugated by lens with interferometer and tested object plane. Instead of pulsed mercury lamp semiconductor laser set in the same casing, wavelength – 532 nm. Incandescent lamp unit saved for both system adjustment and special measurement techniques implementation.

**Interferometer EFL-M70 – IT-183 evolution**

Currently EFL Ltd and INTERFEROMETER Ltd made simulation, design documentation development and now determining the EFL-M70 interferometer next release amount. Interferometer design model is shown in Fig.15.



a



b

Measuring method	Referent and shear interferometry.	
Measuring features	Reflecting surfaces shape and refractive optical components and systems quality control. Gas dynamic medium investigation.	
Testing light beam wavelength, nm	532 / 633	
Aperture, mm	90	
Finite fringe mode error, nm	30	
Spatial-phase mode error, nm	10	
Aspherical surfaces without optical compensators control error, nm	40	
Aspheric surfaces control accuracy from the nearest sphere center, while manufacturing, nm	40	
Focal number	4,5	
Optical zoom range	20:1	
Test surface reflection coefficient range, % *)	4– ≈100	
Number of data processing aberrations programs representation variants*	2	
Dimensions, mm	730x252x254	
Certification and registration as a type in the State Register of approved measuring instruments of Russian Federation		

Fig.15

Figure 15b shows shear unit with IT-183 scheme identical mirrors position in the lower compartment.

\*) Reflection coefficient and wavefront polynomials representation data given rather for optical components and systems control.

Shearing interferometers important difference from other type interferometers seems possibility of the following gas-dynamic medium characteristics quantitative study:

- flow thermodynamic parameters ratio before and after shock wave;

- density inhomogeneity spatial spectrum different intervals;
- turbulent flow statistical characteristics by measuring shear interferogram contrast.

### Conclusion

Features and advantages of the of shear interferometry method in comparison with other gas dynamic medium visualization based optical methods are following:

- 1- Dynamic processes visualization ability often exceeds the shadow methods resolution, and not inferior to the reference wave front interferometry;
- 2- Shearing interferometer systems allows adjusting the sensitivity and dynamic range of the measured parameters in contrast to those mentioned above in paragraph 1;
- 3- Shearing interferometer systems are the most technically realizable in the bench and field studies;
- 4- The possibility to obtain studied gas dynamic medium quantitative characteristics exceeds mentioned above in paragraph 1 systems;
- 5- Shear interferometry systems hardware based on components with minimal technical characteristics requirements, for example, recording camera linearity, image noise presence, illumination inhomogeneity, optical components quality, etc.

### References

- [1] Soroko L. (1981) Gilbert Optics, «Nauka», Moscow.
- [2] Skotnikov M. (1976) Shadow quantitative methods in gas dynamics, "Nauka", Moscow.
- [3] V.N.Shekhtman. (1982) Construction of light wave front from lateral shearing interferograms, Sov.J.Opt. Technology, 49, (10).
- [4] V.N.Shekhtman. A.Yu.Rodionov, A.G.Pel'menev (1994) Reconstruction of a Light Beam Wave Front by Synthesis of a Shear Interferogram, Optics and Spectroscopy, vol.76, No 6, pp.884-888.
- [5] V.N.Shekhtman, A.Yu.Rodionov, A.G.Pel'menev. (1995) Full Reconstruction of a Light Beam Wave Front from a Synthesized Shear Interferogram, vol.79, No 1, pp.124-127.
- [6] V.N.Shekhtman (1998) Synthesis of interferograms by lateral shear to measure wave front of a light beam, Proceeding of the NATO Advanced Research Workshop on Optical Resonators – Theory and Design, Smolenice Castle, Slovak Republic, July 1-5, 1997. Series: Nato Science Partnership Subseries: 3, Vol. 45, Editor » Kossowsky, R. (at al), Kluwer Academic Publishers, Dordrecht/Boston/London, pp. 301-307.
- [7] S.I. Inshakov, A.Yu. Rodionov, A.S. Shirin, V.N. Shekhtman (2011) Interferometer for simultaneous registration two ortogonal directional lateral shear interferograms, *OPTICAL METHODS OF FLOW INVESTIGATION*. Proc. of the 11th International Scientific and Technical Conference OMFI-2011, Moscow.